Research Square

Preprints are preliminary reports that have not undergone peer review.
They should not be considered conclusive, used to inform clinical practice,
or referenced by the media as validated information.

Dapagliflozin prevents contrast-induced acute kidney injury in rats via Nrf2/HO-1-mediated inhibition of NLRP3 inflammation and tubular apoptosis Short Title: Dapagliflozin prevents CI-AKI via Nrf2/HO-1

Zhang Tao
923th Hospital of the Joint Logistics Support Force of PLA
Peng Yumeng
923th Hospital of the Joint Logistics Support Force of PLA
Li Yiyang
littles7@163.com

Minzu Hospital of Guangxi Zhuang Autonomous Region

Article

Keywords: dapagliflozin, Contrast-induced acute kidney injury (CI-AKI), Nrf2/HO-1 pathway, NLRP3 inflammasome, Apoptosis

Posted Date: September 25th, 2026

DOI: https://doi.org/10.21203/rs.3.rs-10925857/v1

License: This work is licensed under a Creative Commons Attribution 4.0 International License. Read Full License

Additional Declarations: No competing interests reported.

Abstract

Contrast-induced acute kidney injury (CI-AKI) is a leading cause of iatrogenic acute kidney injury with limited effective preventive therapies. Dapagliflozin, a sodium-glucose cotransporter 2 inhibitor, has demonstrated pleiotropic renoprotective effects in various kidney diseases, yet its specific mechanism in CI-AKI remains incompletely understood. This study investigated the renoprotective effect of dapagliflozin against CI-AKI and the underlying signaling network. Thirty-six Sprague-Dawley rats were randomly divided into six groups: control, dapagliflozin alone, CI-AKI, CI-AKI plus conventional hydration, CI-AKI plus dapagliflozin pretreatment, and CI-AKI plus dapagliflozin with the HO-1 inhibitor zinc protoporphyrin IX (ZnPP). Renal function parameters, oxidative stress markers, inflammatory mediators, histopathological changes, tubular apoptosis, and expression of Nrf2/HO-1, NLRP3, and AKT/GSK-3β/Caspase-3 pathway-related proteins were evaluated. Dapagliflozin pretreatment significantly improved renal function, attenuated histopathological tubular injury, and reduced tubular apoptosis. Mechanistically, dapagliflozin activated the Nrf2/HO-1 antioxidant pathway, inhibited the NLRP3/IL-1β inflammatory axis, and restored the AKT/GSK-3β survival signaling cascade with downregulation of cleaved caspase-3. Notably, co-administration of ZnPP almost completely abolished these protective effects, indicating that HO-1 serves as an indispensable central hub in dapagliflozin's renoprotective mechanism. Conventional hydration only partially improved renal function with significantly weaker effects on signaling pathways. These findings demonstrate that dapagliflozin exerts multi-mechanism renoprotection against CI-AKI by activating Nrf2/HO-1 as a central hub to synergistically inhibit NLRP3 inflammasome-mediated inflammation and tubular epithelial cell apoptosis, providing new evidence for the potential application of SGLT2 inhibitors in non-diabetic acute kidney injury prevention.

Introduction

Contrast-induced acute kidney injury (CI-AKI), also termed Contrast-induced nephropathy, has emerged as the third leading cause of hospital-acquired acute kidney injury, driven by the widespread application of iodinated contrast media in diagnostic and interventional procedures [1]. Clinically, CI-AKI is defined as an absolute increase in serum creatinine of ≥ 0.5 mg/dL (44.2 μmol/L) or a relative increase of ≥ 25% from baseline within 48–72 hours following intravascular contrast administration, after the exclusion of other identifiable etiologies [2]. The incidence of CI-AKI is particularly high among susceptible populations, including the elderly and patients with chronic kidney disease or diabetes mellitus, with rates reaching up to 40% in certain cohorts [3]. Critically, CI-AKI is independently associated with prolonged hospitalization, increased healthcare costs, and elevated risks of long-term renal dysfunction, dialysis dependence, and mortality (7–31%) [3]. Therefore, the identification of effective preventive strategies represents a critical and unmet clinical need.

The pathogenesis of CI-AKI is multifactorial and complex, involving the synergistic interplay of direct cytotoxicity, hemodynamic alterations, and oxidative stress [4, 5]. Iodinated contrast media directly damage renal tubular epithelial cells and vascular endothelial cells, leading to mitochondrial dysfunction, apoptosis, and necrosis [6]. Concurrently, they induce renal vasoconstriction—particularly within the medulla—resulting in ischemia and hypoxia [7, 8]. This hypoxic milieu exacerbates the production of reactive oxygen species, thereby triggering a cascade of oxidative stress, lipid peroxidation, and inflammatory responses. The nuclear factor erythroid 2-related factor 2 (Nrf2)/heme oxygenase-1 (HO-1) pathway constitutes a pivotal endogenous antioxidant defense system [9, 10]. Meanwhile, the activation of the NOD-like receptor pyrin domain-containing

protein 3 (NLRP3) inflammasome and the subsequent caspase-1-mediated maturation of pro-inflammatory cytokines such as interleukin-1β (IL-1β) are central drivers of sterile inflammation [11, 12]. Ultimately, these converging pathways promote renal tubular epithelial cell apoptosis—a hallmark event in the pathophysiology of CI-AKI—mediated primarily by the activation of executioner caspases such as caspase-3 [6].

Current preventive strategies for CI-AKI remain limited. Although intravenous hydration is the cornerstone and the only universally recommended prophylactic measure [2, 13], the efficacy of various pharmacological interventions—including N-acetylcysteine, statins, and theophylline—remains controversial, with insufficient high-level evidence or strong support from clinical guidelines [3, 4]. This underscores the urgent need for novel therapeutic agents capable of simultaneously targeting the multiple pathological axes of CI-AKI.

Sodium-glucose cotransporter 2 (SGLT2) inhibitors, such as dapagliflozin, are a class of glucose-lowering agents that promote urinary glucose excretion. Beyond their glycemic benefits, large-scale cardiovascular and renal outcome trials have revealed that SGLT2 inhibitors confer significant cardiorenal protection, including a reduced risk of acute kidney injury, in patients with or without type 2 diabetes mellitus [14, 15]. The mechanisms underlying these benefits are pleiotropic, encompassing improvements in tubuloglomerular feedback, reduction of intraglomerular pressure, and anti-inflammatory and anti-fibrotic effects [16, 17]. Notably, preclinical studies have suggested that dapagliflozin may attenuate CI-AKI through the regulation of the HIF-1α/HE4/NF-κB pathway [18], highlighting its potential multi-target mode of action. However, whether dapagliflozin exerts protective effects against CI-AKI through the simultaneous regulation of the antioxidant Nrf2/HO-1 pathway, NLRP3 inflammasome-mediated inflammation, and downstream apoptotic cascades remains to be elucidated.

On the basis of these findings, we hypothesized that dapagliflozin pretreatment would confer renoprotection in a rat model of CI-AKI through a multi-mechanistic approach involving: (1) enhancement of endogenous antioxidant defense via the Nrf2/HO-1 pathway; (2) inhibition of NLRP3 inflammasome activation and IL-1β release; and (3) suppression of renal tubular epithelial cell apoptosis via the caspase-3 pathway. To test this hypothesis, we established a well-validated rat model of CI-AKI and comprehensively evaluated the effects of dapagliflozin on renal function, oxidative stress markers, inflammatory mediators, histopathological changes, and the expression of key proteins in the aforementioned signaling pathways. Furthermore, pharmacological validation was performed using the HO-1 inhibitor zinc protoporphyrin IX (ZnPP) to determine the specific role of the HO-1 pathway in the effects of dapagliflozin. Here, we hypothesized that dapagliflozin pretreatment confers renoprotection against CI-AKI in rats through synergistic activation of the Nrf2/HO-1 pathway, suppression of NLRP3 inflammasome-mediated inflammation, and inhibition of tubular epithelial cell apoptosis. To test this hypothesis, we employed a well-established rat CI-AKI model and evaluated the effects of dapagliflozin on renal function, histopathology, oxidative stress, inflammation, and apoptosis, with pharmacological validation using the HO-1 inhibitor ZnPP.

Materials and Methods

Experimental Animals

A total of 36 specific pathogen-free (SPF) male Sprague-Dawley rats, weighing 180–220 g and aged 6–8 weeks, were purchased from Sipeifu (Beijing) Biotechnology Co., Ltd. (License No.: SCXK (Beijing) 2019-0010).

The animals were housed under standardized conditions at 20–25°C, 40–60% relative humidity, and a 12-h light/dark cycle, with free access to food and water. For anesthesia, rats were injected intraperitoneally with sodium pentobarbital (50 mg/kg). After confirming a surgical plane of anesthesia (loss of pedal withdrawal reflex), euthanasia was performed by exsanguination via aortic transection. Death was confirmed by the cessation of spontaneous respiration and heartbeat.

Drugs and Reagents

Dapagliflozin (AstraZeneca, Lot No.: LP2385); indomethacin and Nω-nitro-L-arginine methyl ester hydrochloride (L-NAME) (Shanghai Macklin Biochemical Technology Co., Ltd.); iopromide injection (Bayer Healthcare Co., Ltd.); and zinc protoporphyrin IX (ZnPP) (Sigma-Aldrich) were used in this study. Assay kits for superoxide dismutase (SOD), malondialdehyde (MDA), blood urea nitrogen (BUN), and creatinine (Cr) were obtained from Nanjing Jiancheng Bioengineering Institute. An enzyme-linked immunosorbent assay (ELISA) kit for interleukin-1β (IL-1β) was purchased from Wuhan Huamei Biotech Co., Ltd. Antibodies against Nrf2, HO-1, NLRP3, p-AKT, AKT, p-GSK-3β, GSK-3β, Caspase-3, Cleaved Caspase-3, and β-actin were all obtained from Cell Signaling Technology.

Experimental Grouping and Establishment of the CI-AKI Model

Rats were randomly assigned into six groups (n = 6 per group) using a random number table: (1) **Control group**; (2) **Dapa group** (dapagliflozin alone); (3) **CI-AKI group**; (4) **CI-AKI + Hyd group** (CI-AKI + hydration); (5) **CI-AKI+Dapa group** (CI-AKI + dapagliflozin); and (6) **CI-AKI+ZnPP+Dapa group** (CI-AKI + ZnPP + dapagliflozin).

The CI-AKI model was established as previously described. Briefly, after 24 hours of water deprivation, rats received sequential tail vein injections of indomethaCI-AKI (10 mg/kg, dissolved in 1.25% sodium bicarbonate), followed 15 minutes later by L-NAME (10 mg/kg, dissolved in normal saline), and then 15 minutes later by iopromide (1600 mg/kg). The Control group received an equivalent volume of normal saline via tail vein injection at the corresponding time points.

For drug intervention, dapagliflozin (1 mg/kg) was administered by oral gavage 2 hours before CI-AKI induction in the Dapa, CI-AKI+Dapa, and CI-AKI+ZnPP+Dapa groups. In the CI-AKI+ZnPP+Dapa group, the HO-1 inhibitor ZnPP (30 mg/kg) was injected intraperitoneally 9 hours before CI-AKI induction. In the CI-AKI + Hyd group, normal saline was continuously infused intravenously (1 mL/kg/h) from 24 hours before to 24 hours after CI-AKI induction. The Control and CI-AKI groups received an equivalent volume of vehicle by oral gavage.

Sample Collection

Forty-eight hours after successful CI-AKI induction, under deep anesthesia, blood was collected from the abdominal aorta, allowed to clot at room temperature, and centrifuged (3500 rpm, 10 min, 4°C). Serum was separated and stored at − 80°C until analysis. Both kidneys were immediately excised; one was fixed in 4% paraformaldehyde for histopathological examination, and the other was snap-frozen in liquid nitrogen and stored at − 80°C for biochemical and molecular analyses.

Assessment of Renal Function

Serum creatinine (Scr) and blood urea nitrogen (BUN) concentrations were measured using an automated biochemical analyzer, strictly following the manufacturer's instructions. Creatinine clearance (Ccr) was calculated based on 24-hour urine volume, urinary creatinine concentration, and serum creatinine concentration.

Evaluation of Oxidative Stress Markers

Frozen kidney tissue was homogenized, and the homogenate was used to determine SOD activity and MDA content to evaluate the level of oxidative stress, according to the protocols provided with the respective commercial assay kits.

Detection of Serum IL-1β by ELISA

The serum level of IL-1β was measured using a commercially available ELISA kit in accordance with the manufacturer's instructions.

Histopathological Examination

Kidney tissues fixed in 4% paraformaldehyde were embedded in paraffin, sectioned at a thickness of 4 μm, and stained with hematoxylin and eosin (H&E). The stained sections were examined under a light microscope for renal tubular injury, including vacuolar degeneration, cast formation, brush border loss, and inflammatory cell infiltration. Semiquantitative scoring of tubular injury was performed by two pathologists who were blinded to the group assignments.

Assessment of Apoptosis by TUNEL Staining

Apoptosis in kidney tissue was detected using the terminal deoxynucleotidyl transferase-mediated dUTP nick-end labeling (TUNEL) assay. After staining, TUNEL-positive cells were observed and counted under a fluorescence microscope, and the apoptotic rate was calculated as the percentage of TUNEL-positive cells relative to the total number of cells.

Western Blot Analysis

Frozen kidney tissue was lysed in RIPA buffer, and total protein concentration was determined using the BCA method. Equal amounts of protein were separated by SDS-PAGE and transferred onto PVDF membranes. After blocking with 5% non-fat milk, the membranes were incubated overnight at 4°C with primary antibodies against Nrf2, HO-1, NLRP3, p-AKT, AKT, p-GSK-3β, GSK-3β, Caspase-3, Cleaved Caspase-3, and β-actin (all at a dilution of 1:1000). The membranes were then incubated with the appropriate horseradish peroxidase-conjugated secondary antibodies for 1 hour at room temperature. Protein bands were visualized using an enhanced chemiluminescence (ECL) reagent and quantified using Image J software. The relative expression levels of target proteins were normalized to those of β-actin (or Lamin B for nuclear proteins).

Immunofluorescence Staining

Paraffin-embedded kidney sections were deparaffinized, subjected to antigen retrieval, and blocked. The sections were then incubated overnight at 4°C with primary antibodies against Nrf2, HO-1, or NLRP3, followed by incubation with fluorescence-conjugated secondary antibodies for 1 hour at room temperature in the dark. Nuclei were counterstained with DAPI. Fluorescence images were captured using a fluorescence microscope, and the mean fluorescence intensity was quantified using Image J software.

Statistical Analysis

All data are presented as mean ± standard deviation (SD). Statistical analyses were performed using SPSS 22.0 software. Differences among multiple groups were compared using one-way analysis of variance (ANOVA), followed by Fisher's least significant difference (LSD) post-hoc test for pairwise comparisons when the assumption of homogeneity of variance was met. A value of $P < 0.05$ was considered statistically significant. All figures were generated using GraphPad Prism 9.0 software.

Results

Renal Function and Histopathological Injury in CI-AKI Rats

To evaluate the renoprotective effects of dapagliflozin against CI-AKI, renal function parameters and renal histomorphological changes were assessed in all experimental groups. As shown in Fig. 1A–C **and** Table 1, rats in the CI-AKI group exhibited significantly elevated serum creatinine (Scr) and blood urea nitrogen (BUN) levels, along with a marked reduction in creatinine clearance rate (Ccr), compared with the Control group (all $P < 0.05$). Pretreatment with dapagliflozin (CI-AKI+Dapa group) markedly reversed these alterations, as evidenced by significantly decreased Scr and BUN levels and increased Ccr (all $P < 0.05$ vs. CI-AKI group). Notably, conventional hydration therapy (CI-AKI + Hyd group) only partially ameliorated Scr and Ccr and exerted a weaker effect on BUN than did dapagliflozin pretreatment. Administration of dapagliflozin alone (Dapa group) had no significant impact on any renal function parameter.

Histopathological examination of kidney tissues by hematoxylin and eosin (H&E) staining **(**Fig. 1D) revealed normal glomerular and tubular architecture in the Control group, with no evidence of tubular injury, hemorrhage, or inflammatory cell infiltration. Similarly, the Dapa group showed only occasional mild glomerular shrinkage without overt pathological changes. In contrast, the CI-AKI group displayed typical features of acute tubular injury, including extensive tubular epithelial cell vacuolar degeneration, brush border loss, cast formation, and interstitial inflammatory cell infiltration. Pretreatment with dapagliflozin markedly attenuated these histopathological alterations, as reflected by relatively preserved tubular architecture and substantially reduced interstitial congestion and inflammatory infiltration. The hydration group also exhibited partial improvement; however, the renal tubular injury score remained significantly higher than that in the CI-AKI+Dapa group (Table 1, $P < 0.05$).

(A–C) Renal function parameters: serum creatinine (Scr, A), blood urea nitrogen (BUN, B), and creatinine clearance rate (Ccr, C) in each group. Data are presented as mean ± SD (n = 6). **(D)** Representative photomicrographs of hematoxylin and eosin (H&E) staining of kidney tissue from each group (original magnification ×200). Scale bars = 100 μm. Black arrows indicate glomeruli; yellow arrows indicate renal

tubules; green arrows indicate degenerated glomeruli or tubules; red arrows indicate inflammatory cell infiltration.

*P < 0.05 vs Control; #P < 0.05 vs CI-AKI; †P < 0.05 vs CI-AKI+Dapa.

Table 1
Renal function parameters and histopathological injury scores

Group	Scr (μmol/L)	Ccr (mL/(min·kg))	BUN (mmol/L)	Interstitial congestion	Protein casts	Tubular necrosis	Total score
Control	29.20 ± 3.69	2.53 ± 0.24	1.54 ± 0.30	0.33 ± 0.58	0.67 ± 0.58	0.00 ± 0.00	1.00 ± 0.00
Dapa	33.12 ± 3.70	2.45 ± 0.20	1.47 ± 0.28	1.00 ± 1.00	1.33 ± 0.58	0.00 ± 0.00	2.33 ± 0.58
CI-AKI	59.95 ± 10.47*	1.87 ± 0.23*	3.94 ± 0.47*	3.00 ± 1.00*	3.33 ± 0.58*	3.67 ± 1.15*	10.00 ± 1.00*
CI-AKI + Hyd	57.92 ± 9.15*	1.90 ± 0.11*	3.58 ± 0.81*	3.33 ± 0.58*	3.67 ± 0.58*	4.33 ± 0.58*	11.33 ± 0.58*
CI-AKI+Dapa	38.79 ± 9.27*#	2.22 ± 0.21*#	2.26 ± 0.46*#	1.67 ± 0.58*#	2.00 ± 0.00*#	1.33 ± 0.58*#	5.00 ± 1.00*#
CI-AKI+ZnPP+Dapa	55.40 ± 8.32*†	1.90 ± 0.18*†	4.37 ± 0.53*†	2.33 ± 0.58*†	2.67 ± 0.58*†	2.00 ± 0.00*†	7.00 ± 1.00*†
F value	20.37	13.273	37.637	10.48	18.92	29.80	83.42
P value	< 0.001	< 0.001	< 0.001	< 0.001	< 0.001	< 0.001	< 0.001

Data are mean ± SD. *n* = 6 for renal function parameters (Scr, Ccr, BUN); *n* = 3 for histopathological scoring. Histopathological items scored 0–5 (0 = normal, 5 = most severe); Total score = sum of three items. P < 0.05 vs. Control; #P < 0.05 vs. CI-AKI; †P < 0.05 vs. CI-AKI+Dapa. Abbreviations: Scr, serum creatinine; Ccr, creatinine clearance rate; BUN, blood urea nitrogen; Dapa, dapagliflozin; ZnPP, zinc protoporphyrin IX.

Nrf2/HO-1 Pathway Activation and Oxidative Stress Attenuation

Oxidative stress is a central pathogenic mechanism in CI-AKI. To evaluate the antioxidant capacity of dapagliflozin, the levels of malondialdehyde (MDA) and superoxide dismutase (SOD) in kidney tissues were measured. As shown in Fig. 2A–B and Table 2, the CI-AKI group exhibited a significantly higher renal MDA content and a markedly lower SOD activity compared with the Control group (all P < 0.05). Dapagliflozin pretreatment (CI-AKI+Dapa group) potently reversed these alterations, as evidenced by reduced MDA levels and restored SOD activity (all P < 0.05 vs. CI-AKI group). In contrast, conventional hydration therapy (CI-AKI + Hyd group) exhibited only limited improvement in these oxidative stress parameters.

To further elucidate the underlying antioxidant mechanism, the activation of the nuclear factor erythroid 2-related factor 2 (Nrf2)/heme oxygenase-1 (HO-1) signaling pathway was examined by Western blot analysis

and immunofluorescence staining. As shown in Fig. 2C–F, the CI-AKI group displayed a modest compensatory increase in nuclear Nrf2 protein expression and its downstream target HO-1 compared with the Control group, reflecting an endogenous adaptive response to oxidative stress. Remarkably, dapagliflozin pretreatment substantially upregulated the protein level and transcriptional activity of nuclear Nrf2 in renal tubular epithelial cells and strongly induced HO-1 protein expression (all $P < 0.05$ vs. CI-AKI group). Immunofluorescence staining further confirmed these findings, demonstrating that the fluorescence intensities of nuclear Nrf2 and HO-1 were markedly elevated in the CI-AKI+Dapa group compared with the CI-AKI group (Fig. 3A–B; Table 2). The CI-AKI + Hyd group showed a moderate increase in Nrf2 and HO-1 expression, albeit to a lesser extent than the CI-AKI+Dapa group. Collectively, these data demonstrate that dapagliflozin potently activates the endogenous Nrf2/HO-1 antioxidant defense pathway in the kidney.

(A–B) Renal oxidative stress parameters: malondialdehyde (MDA) content (A) and superoxide dismutase (SOD) activity (B) in each group. **(C)** Representative Western blot images of nuclear Nrf2 (100 kDa), HO-1 (33 kDa), and NLRP3 (118 kDa) protein expression. Lamin B (66 kDa) and β-actin (42 kDa) served as loading controls for nuclear and cytoplasmic fractions, respectively. **(D–F)** Densitometric quantification of nuclear Nrf2 (D), HO-1 (E), and NLRP3 (F) protein expression relative to loading controls. Data are presented as mean ± SD (n = 6). * $P < 0.05$ vs. Control group; # $P < 0.05$ vs. CI-AKI group; † $P < 0.05$ vs. CI-AKI+Dapa group.

Representative immunofluorescence images (upper panels and lower left panel). Blue fluorescence indicates DAPI nuclear staining, red fluorescence indicates target protein expression, and the merged images show the overlay of both channels. The lower right panel shows the quantification of NRF2, HO-1, and NLRP3 fluorescence intensity. Scale bars = 100 μm. Original magnification ×200. Data are presented as mean ± SD (n = 6). *P < 0.05 vs Control; #P < 0.05 vs CI-AKI.

Table 2
Oxidative stress markers and Nrf2/HO-1 pathway protein expression

Group	MDA (nmol/mg prot)	SOD (U/mg prot)	Nrf2/Lamin B (WB)	HO-1/β-actin (WB)	Nrf2 (IF intensity)	HO-1 (IF intensity)
Control	3.22 ± 0.82	283.90 ± 42.61	0.48 ± 0.12	0.46 ± 0.05	0.35 ± 0.25	3.62 ± 1.15
Dapa	3.48 ± 0.90	277.73 ± 47.32	0.47 ± 0.13#	0.51 ± 0.07#	0.2 ± 0.12#	5.55 ± 1.28 #
CI-AKI	6.31 ± 1.44*	159.77 ± 28.71*	0.7 ± 0.15*	0.68 ± 0.04*	1.6 ± 0.44*	25.16 ± 1.61*
CI-AKI + Hyd	5.72 ± 1.25*	176.40 ± 31.07*	0.68 ± 0.14* #	0.71 ± 0.04*	3.09 ± 0.87*	30.42 ± 0.44*
CI-AKI+Dapa	4.33 ± 0.80*#	228.95 ± 43.98*#	1.17 ± 0.06* #	1.02 ± 0.08* #	17.12 ± 1.1* #	41.03 ± 1.57* #
CI-AKI+ZnPP+Dapa	6.86 ± 1.31*†	148.46 ± 47.12*†	0.88 ± 0.08* #	0.87 ± 0.07* #	1.7 ± 0.22*	22.7 ± 0.98* #
F value	11.190	12.823	30.222	70.487	435.784	517.061
P value	< 0.001	< 0.001	< 0.001	< 0.001	< 0.001	< 0.001

Data are mean ± SD (*n* = 6). WB, Western blotting; IF, immunofluorescence (integrated optical density). MDA, malondialdehyde; SOD, superoxide dismutase; Nrf2, nuclear factor erythroid 2-related factor 2; HO-1, heme oxygenase-1. P < 0.05 vs. Control; #P < 0.05 vs. CI-AKI; †P < 0.05 vs. CI-AKI+Dapa.

NLRP3 Inflammasome Suppression and IL-1β Release

Given that oxidative stress is a potent trigger of inflammatory cascades, we next examined the NLRP3 inflammasome pathway. To assess the effect of dapagliflozin on this pathway, we measured IL-1β protein levels in renal tissues of rats from each group by ELISA. Compared with the Control group, IL-1β levels were significantly elevated in the CI-AKI, CI-AKI+Dapa, CI-AKI + Hyd, and CI-AKI+ZnPP+Dapa groups (P < 0.05). In comparison with the CI-AKI group, the CI-AKI+Dapa group exhibited a significant reduction in IL-1β levels (P < 0.05, Table 3). Collectively, these findings indicate that dapagliflozin pretreatment effectively suppresses NLRP3 inflammasome activation and the subsequent release of downstream IL-1β, thereby attenuating contrast-induced renal inflammatory injury.

Table 3
NLRP3 inflammasome activation and IL-1β release

Group	NLRP3/β-actin (WB)	NLRP3 (IF intensity)	IL-1β (pg/mL, serum)
Control	0.23 ± 0.06	3.57 ± 1.13	41.17 ± 8.75
Dapa	0.25 ± 0.07#	4.25 ± 1.09#	50.69 ± 9.00
CI-AKI	0.66 ± 0.14*	32.49 ± 3.08*	102.61 ± 12.63*
CI-AKI + Hyd	0.71 ± 0.14*	19.3 ± 1.1* #	96.75 ± 12.29*
CI-AKI+Dapa	0.42 ± 0.09* #	13.86 ± 1.76* #	81.76 ± 13.97*#
CI-AKI+ZnPP+Dapa	0.51 ± 0.12* #	32.4 ± 3.19*	105.47 ± 8.88*†
F value	20.891	113.337	36.958
P value	< 0.001	< 0.001	< 0.001

Data are mean ± SD (*n* = 6). NLRP3, NOD-like receptor family pyrin domain containing 3; IL-1β, interleukin-1β. P < 0.05 vs. Control; #P < 0.05 vs. CI-AKI; †P < 0.05 vs. CI-AKI+Dapa.

TUNEL morphologic evidence

Apoptosis of renal tubular epithelial cells directly underlies renal function loss in CI-AKI. To evaluate the anti-apoptotic effect of dapagliflozin, TUNEL staining was first performed (Fig. 4, Table 4). Only scattered TUNEL-positive cells were observed in the Control and Dapa groups (apoptotic rates of 0.88% ± 0.28% and 0.84% ± 0.23%, respectively). In contrast, the CI-AKI group exhibited a sharply elevated apoptotic rate of 25.07% ± 0.45% (P < 0.05 vs. Control), confirming successful induction of tubular apoptosis by contrast media. Notably, dapagliflozin pretreatment (CI-AKI+Dapa group) significantly reduced the apoptotic rate to 4.38% ± 0.34% (P < 0.05 vs. CI-AKI). Hydration therapy (CI-AKI + Hyd group) also conferred partial protection (11.64% ± 0.74%, P < 0.05 vs. CI-AKI), albeit with substantially less potency than dapagliflozin.

Table 4
Renal tubular apoptosis and AKT/GSK-3β survival signaling

Group	TUNEL apoptotic rate (%)	p-AKT/AKT	p-GSK-3β/GSK-3β	Cleaved Caspase-3/Caspase-3
Control	0.88 ± 0.28	1.22 ± 0.37	1.04 ± 0.09	0.2 ± 0.08
Dapa	0.84 ± 0.23#	1.18 ± 0.28#	1.02 ± 0.13#	0.22 ± 0.09#
CI-AKI	25.07 ± 0.45*	0.48 ± 0.19*	0.36 ± 0.04*	0.32 ± 0.13*
CI-AKI + Hyd	11.64 ± 0.74*#	0.85 ± 0.26*#	0.62 ± 0.05*#	0.25 ± 0.1*#
CI-AKI+Dapa	4.38 ± 0.34*#	1 ± 0.31#	0.75 ± 0.07*#	0.25 ± 0.1*#
CI-AKI+ZnPP+Dapa	27.13 ± 1.03*#	0.53 ± 0.22*#	0.33 ± 0.04*	0.28 ± 0.12*#
F	1238.117	7.801	99.185	13.269
P	< 0.001	0.001	< 0.001	< 0.001

Data are mean ± SD (*n* = 6). TUNEL apoptotic rate = percentage of TUNEL-positive nuclei. AKT, protein kinase B; GSK-3β, glycogen synthase kinase-3β; Cleaved Caspase-3/Caspase-3 ratio reflects activation of the apoptotic executioner cascade. P < 0.05 vs. Control; #P < 0.05 vs. CI-AKI; †P < 0.05 vs. CI-AKI+Dapa.

Representative fluorescence images (×200): blue indicates DAPI-stained nuclei, and green indicates TUNEL-positive cells (apoptotic cells). The bar chart below shows the quantitative analysis of the apoptotic rate in each group (n = 6). *P < 0.05 vs. Control; #P < 0.05 vs. CI-AKI; †P < 0.05 vs. CI-AKI+Dapa.

Molecular mechanisms via Western blotting

To further explore the underlying molecular machinery, we examined the apoptotic executioner Cleaved Caspase-3 and the AKT/GSK-3β survival signaling pathway by Western blotting (Fig. 5, Table 4). Compared with the Control group, the CI-AKI group displayed a markedly elevated Cleaved Caspase-3/Caspase-3 ratio (0.32 ± 0.13 vs. 0.20 ± 0.08, P < 0.05), alongside significantly reduced p-AKT/AKT (0.48 ± 0.19) and p-GSK-3β/GSK-3β (0.36 ± 0.04) ratios (both P < 0.05 vs. Control), indicating suppression of pro-survival signaling and activation of the apoptotic cascade. Dapagliflozin pretreatment substantially reversed these alterations: the Cleaved Caspase-3/Caspase-3 ratio decreased to 0.25 ± 0.10 (P < 0.05 vs. CI-AKI), whereas p-AKT/AKT (1.00 ± 0.31) and p-GSK-3β/GSK-3β (0.75 ± 0.07) ratios were significantly upregulated (both P < 0.05 vs. CI-AKI). Hydration therapy improved these parameters to a lesser degree (p-AKT/AKT: 0.85 ± 0.26; p-GSK-3β/GSK-3β: 0.62 ± 0.05; Cleaved Caspase-3: 0.25 ± 0.10). Importantly, in the CI-AKI+ZnPP+Dapa group, the dapagliflozin-induced activation of the AKT/GSK-3β pathway was markedly blunted (p-AKT/AKT: 0.53 ± 0.22; p-GSK-3β/GSK-3β: 0.33 ± 0.04; both P < 0.05 vs. CI-AKI+Dapa), and the Cleaved Caspase-3/Caspase-3 ratio (0.28 ± 0.12) rebounded to near CI-AKI levels.

Taken together, these TUNEL and Western blot findings demonstrate that dapagliflozin suppresses Caspase-3 activation via AKT/GSK-3β-dependent survival signaling, thereby substantially reducing tubular epithelial

apoptosis.

(A) Representative Western blot bands. (B) Quantitative analysis of the p-AKT/AKT ratio. (C) Quantitative analysis of the p-GSK-3β/GSK-3β ratio. (D) Quantitative analysis of the Cleaved Caspase-3 ratio. Data are presented as mean ± SD (n = 6). *P < 0.05 vs. Control; #P < 0.05 vs. CI-AKI.

Pharmacological Reverse Validation of the Nrf2/HO-1 Pathway with ZnPP

To validate the central role of the Nrf2/HO-1 pathway in the renoprotective effects of dapagliflozin, we employed the specific HO-1 inhibitor zinc protoporphyrin IX (ZnPP) for pharmacological reverse validation. As summarized in Tables 1–4, ZnPP administration effectively reversed the protective effects of dapagliflozin across all measured parameters, with each indicator returning to levels comparable to those in the CI-AKI model group. Specifically, ZnPP reversed the beneficial effects of dapagliflozin on serum creatinine, blood urea nitrogen, and creatinine clearance rate, and restored the renal tubular injury score to a level resembling that of the CI-AKI group. Concurrently, ZnPP completely abolished the modulatory effects of dapagliflozin on malondialdehyde and superoxide dismutase, and significantly suppressed dapagliflozin-induced HO-1 protein overexpression. Furthermore, ZnPP treatment attenuated the inhibitory effects of dapagliflozin on the NLRP3/IL-1β axis, partially reversed its anti-apoptotic effects, and blunted the upregulation of phosphorylated AKT and phosphorylated GSK-3β.

Collectively, these results unveil a multi-mechanistic synergistic protective network centered on the Nrf2/HO-1 pathway as a core hub. Through the activation of HO-1, dapagliflozin concurrently achieves antioxidant, anti-inflammatory, and anti-apoptotic effects, with these three components being interconnected and mutually reinforcing—the alleviation of oxidative stress may further suppress NLRP3 inflammasome activation, while the improvement of the inflammatory milieu reduces the triggering of apoptotic signaling. The complete reversal of all these protective effects by ZnPP confirms the indispensability of HO-1 within this network. These findings will be discussed in greater detail in the following section.

Discussion

The present study demonstrates, for the first time, that dapagliflozin confers renoprotection against CI-AKI through a multi-mechanistic synergistic network centered on the Nrf2/HO-1 pathway. Using pharmacological reverse-validation with the specific HO-1 inhibitor ZnPP, we establish that HO-1 activation is not a concomitant event but an indispensable hub through which dapagliflozin coordinates antioxidant, anti-inflammatory, and anti-apoptotic effects. These findings extend the current understanding of SGLT2 inhibitors beyond their metabolic and hemodynamic actions, positioning dapagliflozin as a promising mechanism-based prophylactic strategy for CI-AKI—a condition for which effective pharmacological interventions remain conspicuously lacking.

The Nrf2/HO-1 pathway as the central hub of renoprotection

The most compelling evidence derives from the ZnPP reverse-validation experiment. ZnPP, a competitive inhibitor of HO-1 enzymatic activity, not only abrogated dapagliflozin-induced HO-1 overexpression but, more

critically, simultaneously reversed all functional and molecular benefits—including improvements in renal function, histopathology, oxidative stress, NLRP3 inflammasome activation, and tubular apoptosis. This near-complete phenotypic reversion unequivocally establishes HO-1 as the common downstream effector through which dapagliflozin orchestrates its pleiotropic protective actions.

Mechanistically, SGLT2 inhibitors are known to ameliorate renal tissue hypoxia by reducing proximal tubular workload and oxygen consumption—a metabolic shift that may relieve hypoxia-induced suppression of Nrf2 nuclear translocation. While the modest compensatory Nrf2 upregulation observed in the CI-AKI group reflects an endogenous stress response that was insufficient to counter the oxidative insult, dapagliflozin potently amplified this defense program, suggesting augmentation of both the amplitude and duration of Nrf2 activation. The downstream products of HO-1 catalysis—carbon monoxide, biliverdin/bilirubin, and free iron—possess well-established antioxidant, vasodilatory, and cytoprotective properties, providing a plausible mechanistic link between HO-1 activation and the broad-spectrum protection observed.

Interconnected suppression of inflammation and apoptosis

Oxidative stress serves as a principal trigger for NLRP3 inflammasome assembly and IL-1β maturation. Our data reveal that dapagliflozin, while enhancing Nrf2/HO-1-mediated antioxidant capacity, significantly suppressed both NLRP3 expression and IL-1β release. This observation aligns with the emerging concept that HO-1 metabolites directly inhibit NLRP3 activation, possibly through modulation of mitochondrial reactive oxygen species or NF-κB signaling. Thus, the antioxidant and anti-inflammatory effects are not independent but mutually reinforcing: alleviation of oxidative stress curtails the inflammatory trigger, while suppression of the inflammatory milieu attenuates further ROS generation, breaking the vicious cycle that drives CI-AKI progression.

With respect to apoptosis, dapagliflozin not only downregulated executioner caspase-3 but also upregulated the AKT/GSK-3β survival axis—a pathway that integrates pro-survival signals and inhibits pro-apoptotic effectors. Notably, the protective effect on AKT/GSK-3β phosphorylation was largely reversed by ZnPP, indicating that this survival signaling lies downstream of, or is functionally dependent upon, HO-1 activation. This aligns with reports that HO-1-derived carbon monoxide activates PI3K/AKT signaling, providing a direct mechanistic bridge between the antioxidant hub and the anti-apoptotic cascade. Collectively, our data support a model in which HO-1 serves as a molecular switch coordinating a tripartite defense program: quenching oxidants, curbing inflammation, and sustaining cell survival.

Implications for clinical practice: beyond hydration

Intravenous hydration—the current cornerstone of CI-AKI prophylaxis—acts through passive dilution and diuresis without actively engaging endogenous cytoprotective pathways. Our comparative analysis reveals that although hydration partially ameliorated renal dysfunction and histopathology, it was markedly inferior to dapagliflozin in upregulating Nrf2/HO-1, suppressing NLRP3/IL-1β, or activating AKT survival signaling. This differential efficacy underscores a paradigm shift: hydration addresses the physical/pharmacokinetic determinants of contrast nephrotoxicity (contrast concentration and transit time), whereas dapagliflozin targets the biological/cellular determinants (oxidative stress, inflammation, apoptosis). We propose that a combined strategy incorporating dapagliflozin into standard hydration protocols may offer superior renal

protection in high-risk patients through synergy between "flushing" and "cytoprotection"—a hypothesis that warrants rigorous clinical testing.

Limitations and future directions

Several limitations merit acknowledgment. First, while we have established the centrality of HO-1 via ZnPP inhibition, the precise molecular crosstalk between HO-1 and downstream effectors—particularly how HO-1 metabolites specifically modulate NLRP3 inflammasome assembly and AKT phosphorylation—requires further elucidation using co-immunoprecipitation or pathway-specific knockout models. Second, our prophylactic regimen aligns with pre-procedural pharmacoprophylaxis but does not address whether dapagliflozin retains therapeutic efficacy once CI-AKI is established. Third, although ZnPP provided strong pharmacological evidence, we cannot exclude off-target effects; complementary genetic approaches (e.g., tubular-specific HO-1 knockdown) would strengthen our conclusions. Fourth, differences between this rat model and human patients with comorbidities warrant cautious extrapolation, though the low hypoglycemic risk of dapagliflozin in non-diabetic populations is reassuring.

Future investigations should prioritize: (1) exploring the therapeutic window of dapagliflozin in post-exposure settings; (2) validating the hydration-plus-dapagliflozin combination in large-animal and translational models; and (3) employing unbiased proteomic or transcriptomic approaches to identify additional upstream regulators and downstream effectors within the Nrf2/HO-1 network.

Conclusion

In summary, this study demonstrates that dapagliflozin pretreatment exerts robust renoprotection against CI-AKI through a Nrf2/HO-1-centered, multi-mechanistic synergistic network integrating antioxidant, anti-inflammatory, and anti-apoptotic actions. The complete reversal of these protective effects by the HO-1 inhibitor ZnPP establishes HO-1 as an indispensable therapeutic target for CI-AKI. These findings provide a mechanistic rationale for the clinical evaluation of dapagliflozin as a novel prophylactic agent in high-risk patients undergoing contrast-enhanced procedures and open new avenues for mechanism-guided combination strategies beyond conventional hydration.

Declarations

Competing interests

The authors declare no competing interests.

Ethics declarations

All experimental procedures were conducted in accordance with the guidelines for the care and use of laboratory animals, and this study was approved by the Animal Ethics Committee of Minzu Hospital of Guangxi Zhuang Autonomous Region (Ethics Approval No.: Guimin Yilun Shen Tong Zi (2022) No. 42).

Consent for publication

Not applicable.

Funding

This study is supported by Self-funded Research Project of the Health Commission of Guangxi Zhuang Autonomous Region (Z20210583)

Author Contribution

Zhang Tao, Peng Yumeng, and Li Yiyang contributed equally to this work. Zhang Tao: Conceptualization, Methodology, Investigation, Formal analysis, Writing – original draft, Visualization. Peng Yumeng: Methodology, Investigation, Validation, Data curation, Writing – review & editing. Li Yiyang: Conceptualization, Supervision, Project administration, Funding acquisition, Writing – review & editing.

Acknowledgements

We express our great gratitude to all the participants in the present study.

Data Availability

Upon reasonable request, the corresponding author can provide access to the data supporting the findings of this study.

References

1. Zhou, L. Y. et al. Arginase2 mediates contrast-induced acute kidney injury via facilitating nitrosative stress in tubular cells. *Redox Biol.* **67**, 102929 (2023).
2. Pm, P. et al. KDOQI US commentary on the 2012 KDIGO clinical practice guideline for acute kidney injury. *American J. kidney diseases: official J. Natl. Kidney Foundation* **61**, (2013).
3. Y, L. & J, W. Contrast-induced acute kidney injury: a review of definition, pathogenesis, risk factors, prevention and treatment. *BMC nephrology* **25**, (2024).
4. M, F. & Pb, P. E, S., A, P. Understanding and preventing contrast-induced acute kidney injury. *Nature reviews Nephrology* **13**, (2017).
5. As, C. & X, L. The Potential Biotherapeutic Targets of Contrast-Induced Acute Kidney Injury. *International J. Mol. sciences* **24**, (2023).
6. C, Q. et al. In vivo and in vitro assessment of pathways involved in contrast media-induced renal cells apoptosis. *Cell death & disease* **2**, (2011).
7. Mm, S. Pathophysiology of renal tissue damage by iodinated contrast media. *Clinical experimental Pharmacol. & physiology* **38**, (2011).

8. S, B. & Rn, P. Pathophysiology of Contrast-Induced Acute Kidney Injury. *Interventional Cardiol. clinics* **9**, (2020).
9. Mj, U., Eh, K., Ma, H. & H, H. Pharmacotherapy against Oxidative Stress in Chronic Kidney Disease: Promising Small Molecule Natural Products Targeting Nrf2-HO-1 Signaling. *Antioxidants (Basel, Switzerland)* 10, (2021).
10. Wang, W. et al. Berberine alleviates contrast-induced nephropathy by activating Akt/Foxo3a/Nrf2 signalling pathway. *J. Cell. Mol. Med.* **28**, e18016 (2024).
11. Shen, J. et al. NLRP3 inflammasome mediates contrast media-induced acute kidney injury by regulating cell apoptosis. *Sci. Rep.* **6**, 34682 (2016).
12. X, T. et al. Involvement of S100A8/A9-TLR4-NLRP3 Inflammasome Pathway in Contrast-Induced Acute Kidney Injury. *Cellular Physiol. biochemistry: Int. J. experimental Cell. Physiol. Biochem. pharmacology* **43**, (2017).
13. Chandiramani, R., Cao, D., Nicolas, J. & Mehran, R. Contrast-induced acute kidney injury. *Cardiovasc. Interv Ther.* **35**, 209–217 (2020).
14. O, M. et al. Effects of dapagliflozin on development and progression of kidney disease in patients with type 2 diabetes: an analysis from the DECLARE-TIMI 58 randomised trial. *The lancet Diabetes & endocrinology* **7**, (2019).
15. Hjl, H. et al. Dapagliflozin in Patients with Chronic Kidney Disease. *The New. Engl. J. medicine* **383**, (2020).
16. Mazzieri, A. & Marcon, L. M. R. Nephroprotective Mechanisms of SGLT2i: Beyond the Glucose-Lowering Effect. *Biomedicines* **13**, 2123 (2025).
17. X, C., Cf, H., Bk, L. S. & B, H. K. Reno- and cardioprotective molecular mechanisms of SGLT2 inhibitors beyond glycemic control: from bedside to bench. *American J. Physiol. Cell. physiology* **325**, (2023).
18. X, H. et al. Dapagliflozin Attenuates Contrast-induced Acute Kidney Injury by Regulating the HIF-1α/HE4/NF-κB Pathway. *Journal Cardiovasc. pharmacology* **79**, (2022).

Figures

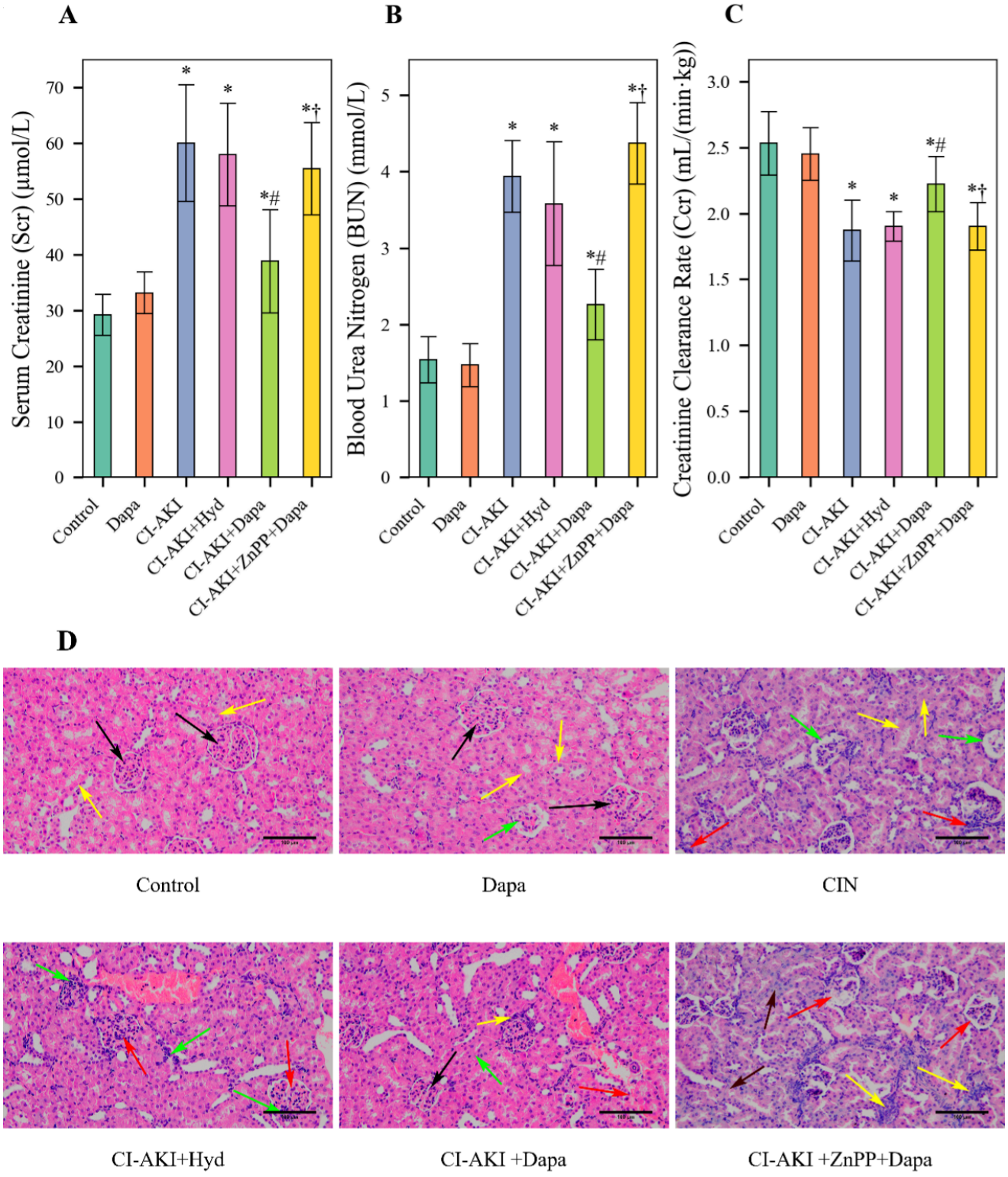


Figure 1

Effects of dapagliflozin on renal function and renal histopathology in CI-AKI rats.
(A–C) Renal function parameters: serum creatinine (Scr, A), blood urea nitrogen (BUN, B), and creatinine clearance rate (Ccr, C) in each group. Data are presented as mean ± SD (n=6). **(D)** Representative photomicrographs of hematoxylin and eosin (H&E) staining of kidney tissue from each group (original magnification ×200). Scale bars = 100 μm. Black arrows indicate glomeruli; yellow arrows indicate renal

tubules; green arrows indicate degenerated glomeruli or tubules; red arrows indicate inflammatory cell infiltration.

*P< 0.05 vs Control; #P < 0.05 vs CI-AKI; †P < 0.05 vs CI-AKI+Dapa.

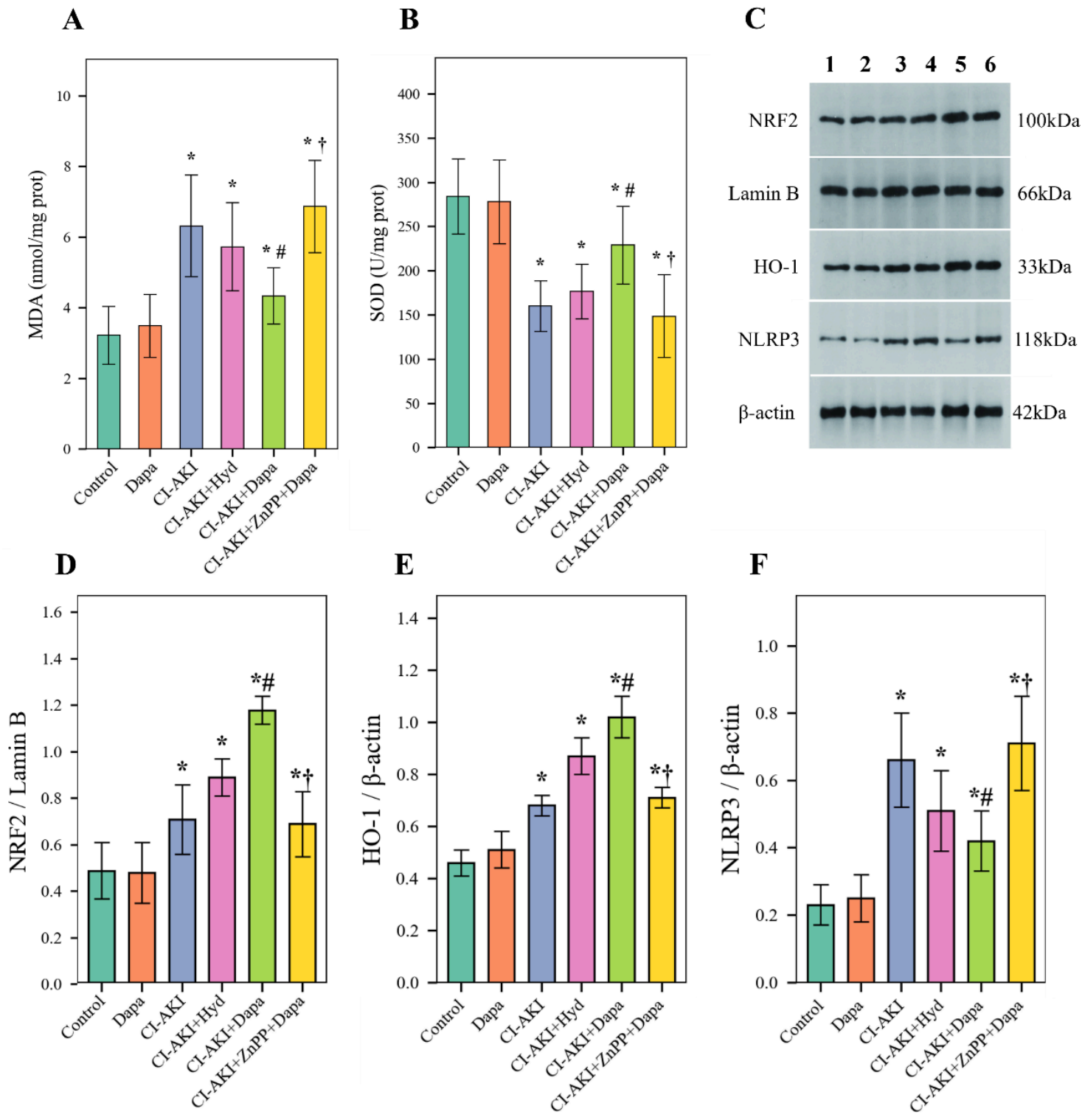


Figure 2

Effects of dapagliflozin on oxidative stress markers and Nrf2/HO-1 pathway protein expression in the kidneys of CI-AKI rats.

(A–B) Renal oxidative stress parameters: malondialdehyde (MDA) content (A) and superoxide dismutase (SOD) activity (B) in each group. **(C)** Representative Western blot images of nuclear Nrf2 (100 kDa), HO-1 (33 kDa), and NLRP3 (118 kDa) protein expression. Lamin B (66 kDa) and β-actin (42 kDa) served as loading controls for nuclear and cytoplasmic fractions, respectively. **(D–F)** Densitometric quantification of nuclear Nrf2 (D), HO-1 (E), and NLRP3 (F) protein expression relative to loading controls. Data are presented as mean ± SD (n = 6). * *P* < 0.05 vs. Control group; # *P* < 0.05 vs. CI-AKI group; † *P* < 0.05 vs. CI-AKI+Dapa group.

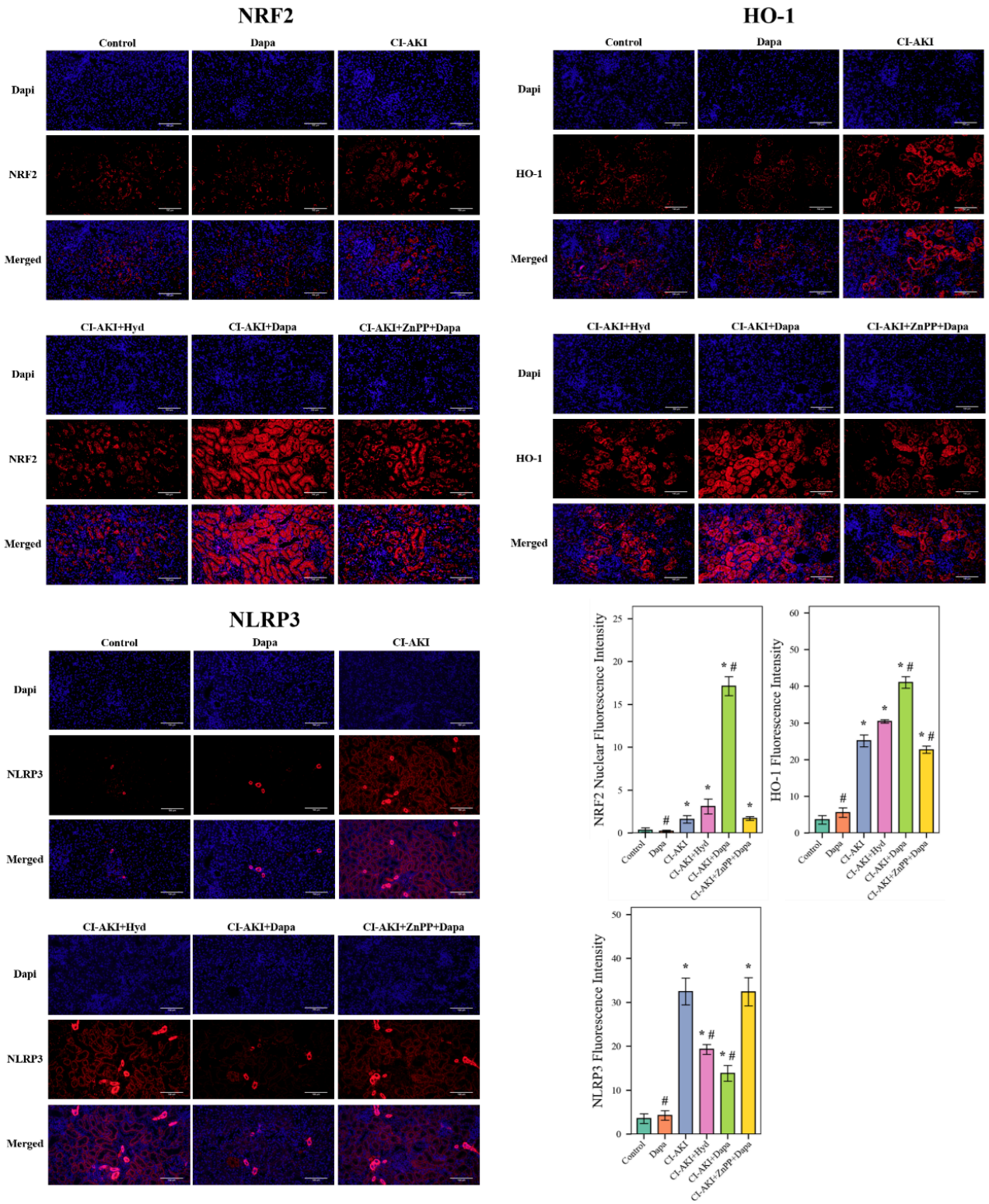


Figure 3

Immunofluorescence expression of Nrf2/HO-1 pathway protein in kidney tissues of CI-AKI rats.

Representative immunofluorescence images (upper panels and lower left panel). Blue fluorescence indicates DAPI nuclear staining, red fluorescence indicates target protein expression, and the merged images show the overlay of both channels. The lower right panel shows the quantification of NRF2, HO-1, and NLRP3 fluorescence intensity. Scale bars = 100 μm. Original magnification ×200. Data are presented as mean ± SD (n = 6). *P < 0.05 vs Control; #P < 0.05 vs CI-AKI.

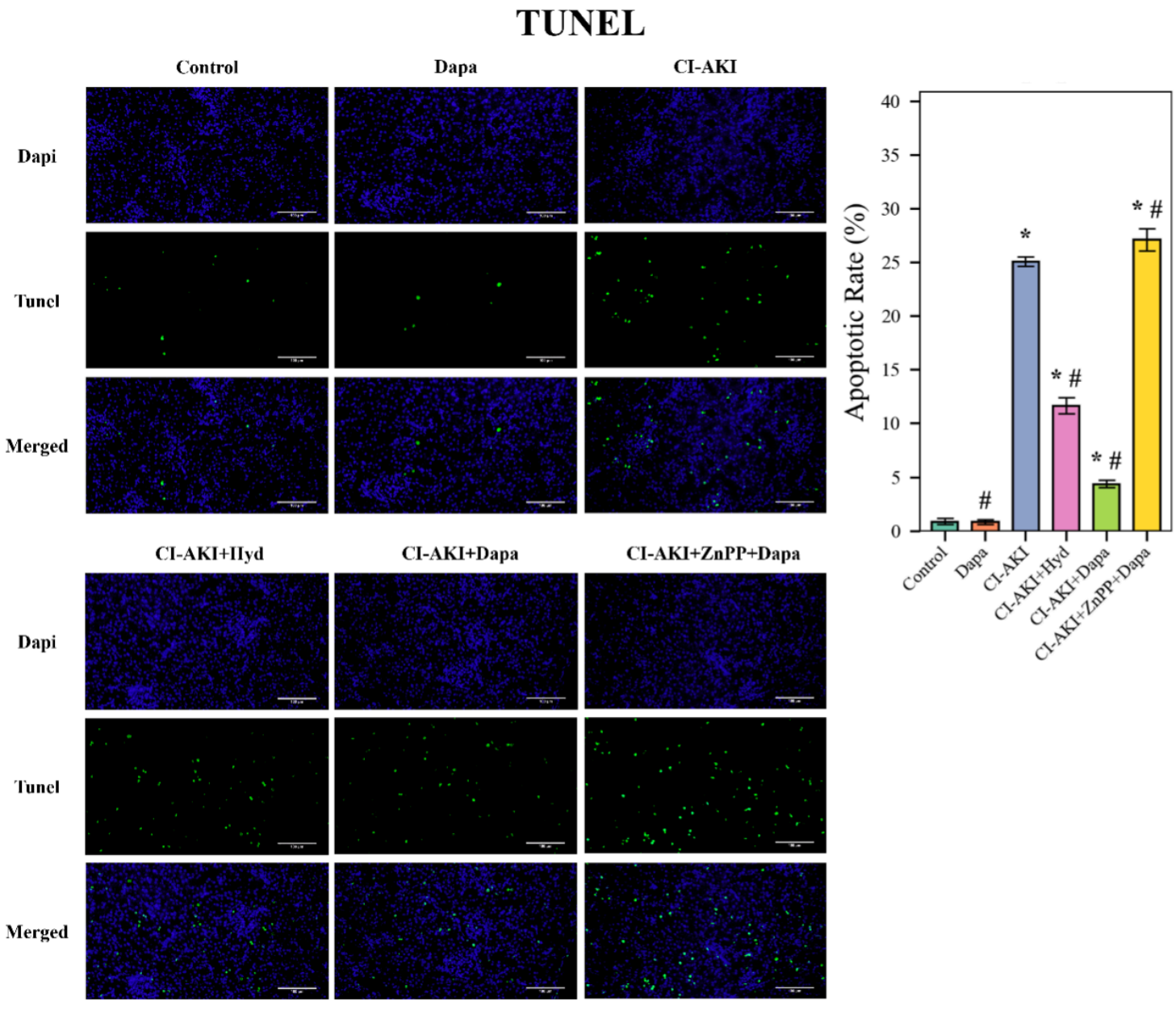


Figure 4

Comparison of TUNEL staining results in renal tissues of rats among groups

Representative fluorescence images (×200): blue indicates DAPI-stained nuclei, and green indicates TUNEL-positive cells (apoptotic cells). The bar chart below shows the quantitative analysis of the apoptotic rate in each group (n = 6). *P < 0.05 vs. Control; #P < 0.05 vs. CI-AKI; †P < 0.05 vs. CI-AKI+Dapa.

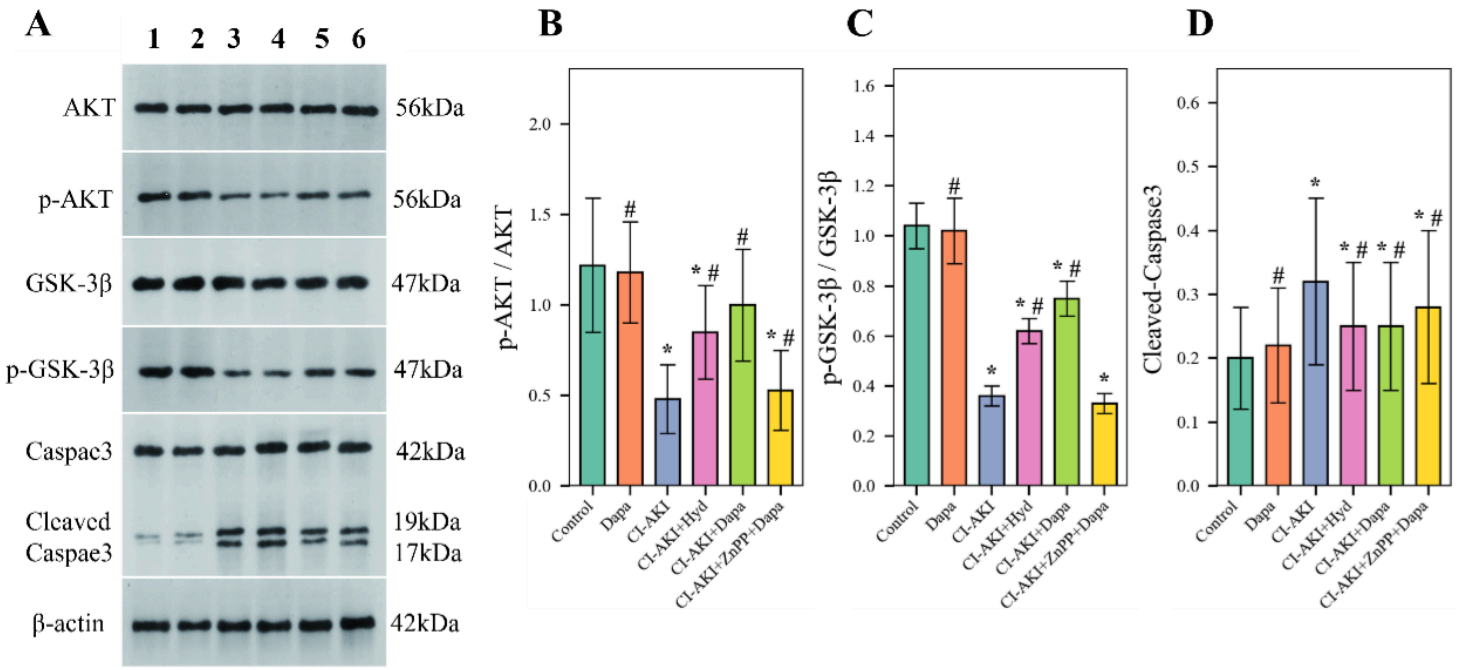


Figure 5

Western blot analysis of apoptosis-related proteins in renal tissues of rats among groups

(A) Representative Western blot bands. (B) Quantitative analysis of the p-AKT/AKT ratio. (C) Quantitative analysis of the p-GSK-3β/GSK-3β ratio. (D) Quantitative analysis of the Cleaved Caspase-3 ratio. Data are presented as mean ± SD (n = 6). *P < 0.05 vs. Control; #P < 0.05 vs. CI-AKI.

Supplementary Files

This is a list of supplementary files associated with this preprint. Click to download.

- SupplementaryInformation.pdf